Colorless Optical Transmitter for Upstream WDM PON Based on Wavelength Conversion

Zaineb Al-Qazwini, *Student Member, IEEE*, Madhan Thollabandi, *Member, IEEE*, and Hoon Kim, *Senior Member, IEEE*

***Abstract*—We propose and demonstrate a novel colorless optical transmitter based on all-optical wavelength conversion using a reflective semiconductor optical amplifier (RSOA) for upstream transmission in wavelength-division-multiplexed passive optical networks. The proposed colorless optical transmitter for the optical network unit is composed of an electro-absorption modulated laser (EML), an optical coupler, and an RSOA. Through cross-gain modulation in the RSOA, the upstream data from the EML pump light are imposed onto a continuous-wave probe light provided from the central office (CO). An optical delay interferometer at the CO tailors the chirp of the upstream signal to improve the bandwidth of the system and dispersion tolerance. The proposed upstream optical transmitter is based on the fast gain recovery of the RSOA governed by carrier-carrier scattering and carrier-phonon interactions. Thus, it can potentially operate at >10 Gb/s. Two separate wavelength bands are allocated, one for the pump signals and the other for the probe signals. Therefore, the proposed transmitter operates in a colorless manner since the EML can have any arbitrary wavelength within the pump band. We demonstrate the transmission of a 10.7-Gb/s upstream signal generated by the proposed scheme in a single-fiber loopback-configured network. The conditions for colorless operation of the proposed transmitter are investigated through experiment.**

***Index Terms*—Passive optical network, semiconductor optical amplifier, wavelength conversion, wavelength-division-multiplexing.**

I. Introduction

HIGH bandwidth applications such as storage networking, video streaming/sharing, and online gaming continue to drive greater bandwidth demands for next-generation broadband access networks. To address the growing capacity, security, and distance requirements while leveraging the benefits of a passive infrastructure, wavelength-division-multiplexed (WDM) passive optical networks (PONs) are considered to be the most scalable and future-proof solution. A key advantage of WDM PONs is the assignment of dedicated wavelength channels to each optical network unit (ONU) while having double-star architecture. This not only guarantees large capacity and high security for each ONU, but also facilitates graceful upgradability and network flexibility [1]–[3]. These merits notwithstanding, WDM PONs are still considered prohibitively expensive due to the high installation, operation, and maintenance costs associated with the upstream wavelength-specific light sources required at the subscribers' premises.

To lower the cost and make WDM PONs a viable solution for broadband access networks, it is highly desirable to utilize colorless optical transmitters at the ONUs for upstream transmission. Identical optical transmitters which operate at any wavelength can be used for any ONUs to substantially lower the operation cost and consequently alleviate the inventory management issue. For this purpose, a couple of optical transmitters based on reflection-type opto-electronic devices, such as reflective semiconductor optical amplifier (RSOA) and incoherent light-injected Fabry-Perot laser diode, have been reported [4], [5]. In this approach, the reflection-type devices operate in a colorless manner by imposing upstream data on the incoming seed light from the central office (CO). Therefore, the wavelength-specific light sources can be all located at the CO, providing service providers with centralized management of the failure-prone light sources. However, the modulation bandwidth of the reflection-type opto-electronic devices is typically limited to less than 2 GHz by the carrier lifetime, which in turn, limits the upstream data rate in these schemes to <2.5 Gb/s [6], [7]. Thus, it is very challenging to operate these low-bandwidth devices at 10 Gb/s and beyond without the assistance of advanced modulation formats [8]–[11], post-detection electrical signal processing [12]–[14], or optical filtering with electrical equalization [15].

In this paper, we propose and demonstrate a novel approach to a colorless optical transmitter based on wavelength conversion. A high-speed optical signal generated from an electro-absorption modulated laser (EML) at the ONU is first wavelength-converted to the wavelength of the seed light by cross-gain modulation (XGM) in a gain-saturated RSOA. Then, a detuned delay interferometer (DI) is used at the CO to improve the bandwidth of the system [16]. In this approach, the RSOA is simply DC-biased without any data modulation. Therefore, the upstream data rate is not limited by the carrier lifetime of the RSOA, but by fast gain recovery governed by carrier-carrier scattering and carrier-phonon interactions. We experimentally demonstrate the transmission of 10-Gb/s upstream data over 20-km standard-single mode fiber (SSMF), investigate the dispersion-induced penalty, and study the conditions for colorless operation in the proposed scheme.

Manuscript received June 29, 2012; revised November 27, 2012; accepted January 02, 2013. Date of publication January 09, 2013; date of current version January 23, 2013. This work was supported in part by Singapore Ministry of Education Academic Research Fund Tier 1.

The authors are with Department of Electrical and Computer Engineering, National University of Singapore, 117583 Singapore (e-mail: hoonkim@ieee.org).

Color versions of one or more of the figures in this letter are available online at http://ieeexplore.ieee.org.

Digital Object Identifier 10.1109/JLT.2013.2238216

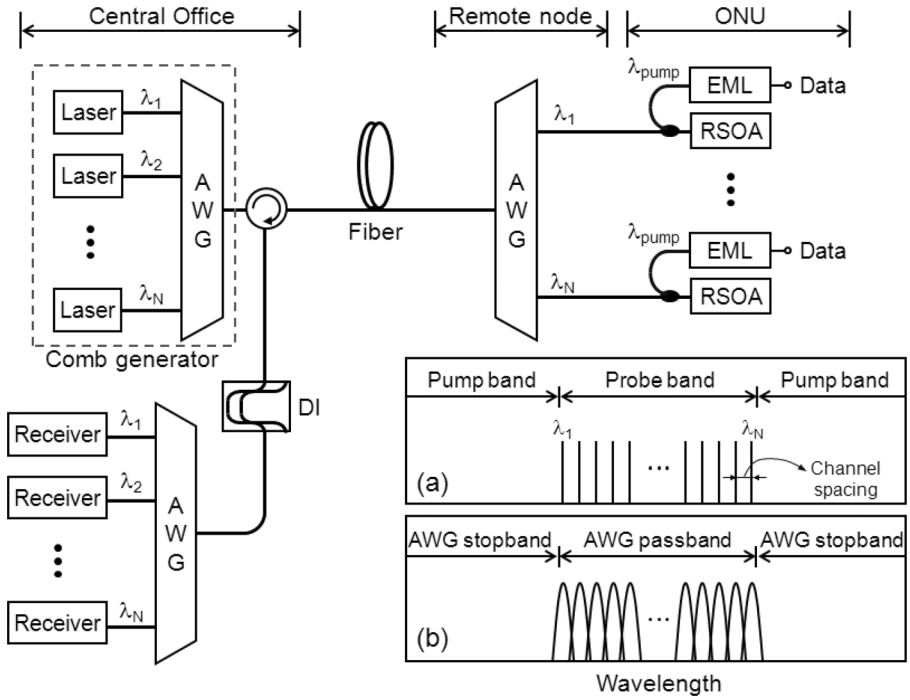

Fig. 1. The schematic diagram of an upstream WDM-PON system utilizing the proposed transmitter based on wavelength conversion. The insets show (a) an example of the wavelength band allocation for the pump and probe signals and (b) AWG spectrum of passband and stopband. AWG: arrayed waveguide grating, DI: delay interferometer, EML: electro-absorption modulated laser, ONU: optical network unit, and RSOA: reflective semiconductor optical amplifier.

The remaining parts of this paper are organized as follows. In Section II, we describe the architecture and the principle of operation of the proposed upstream transmitter. The experimental demonstration and the discussion of the experimental results are presented in Section III. Finally, this paper is summarized in Section IV.

II. Architecture and Principle of Operation

The schematic diagram of an upstream WDM-PON system utilizing the proposed transmitter is illustrated in Fig. 1. A comb generator, which is, for example, composed of wavelength-division-multiplexed wavelength-specific laser diodes as shown in the figure, provides continuous wave (CW) light from λ_1 to $\lambda_{\rm N}$ to N ONUs, where N is the number of channels, through the feeder fiber. This CW light serves to be injected into the RSOAs at the ONUs as seed light and is also referred to as a probe signal in this paper. At the ONU, an EML first generates a non-return-to-zero (NRZ) upstream optical signal at wavelength $\lambda_{\rm pump}$. The EML output (also referred to as a pump signal) is coupled to the CW seed light supplied from the CO and then sent to the RSOA where the wavelength conversion is performed. The upstream data of the pump light are imprinted onto the CW seed light through the XGM where the gain variation of the pump signal modulates the co-propagating CW light [17]–[19]. Since the presence of the pump signal compresses the gain of the RSOA, we have an inverted data pattern after the wavelength conversion [19]. The modulated probe signals ranging from λ_1 to $\lambda_{\rm N}$ are then multiplexed at the remote node and sent back to the CO for detection.

At the CO, the upstream signals are first sent to a DI before being demultiplexed by an arrayed waveguide grating (AWG). The DI which filters out the red-shifted chirp of the converted signal substantially improves the receiver sensitivity and dispersion tolerance [16]. A single DI can be used to equalize multiple WDM channels provided that the free-spectral range (FSR) of the DI is equal to a factor of the channel spacing [20].

It should be noted that in the proposed scheme both the probe and pump signals propagate back to the CO and thus it is necessary to filter out the pump signal using optical filters. To avoid using additional optical filters on the link, we can utilize non-cyclic AWGs at the remote node and at the CO. In this case, $\lambda_{\rm pump}$, the wavelength of the pump signal, should be assigned outside the AWG passband. As shown in Fig. 1(a) and (b), we have two wavelength bands within the RSOA gain spectrum, one for the probe channels and the other for the pump signals. The probe band falls exactly on the AWG passband so that the wavelength-converted probe signal can reach the CO for detection. However, the pump signal, the wavelength of which can be any wavelength outside the AWG passband, is filtered out by two AWGs, one at the remote node and the other at the CO. Note that the proposed wavelength-conversion-based transmitter operates in a colorless manner as long as the EML has any arbitrary wavelength within the pump band region. Thus, identical optical transmitters which satisfy the above band allocation requirements can be used for any ONUs in the proposed scheme. Our allocation scheme can suppress the pump signal by >50 dB since typical commercial non-cyclic AWGs have non-adjacent channel crosstalk better than 25 dB [21].

Fig. 1 illustrates the upstream transmission only. In the proposed network, the downstream data could be accommodated by allocating additional waveband for downstream transmission. In this case, we need to employ at the remote node a multi-band

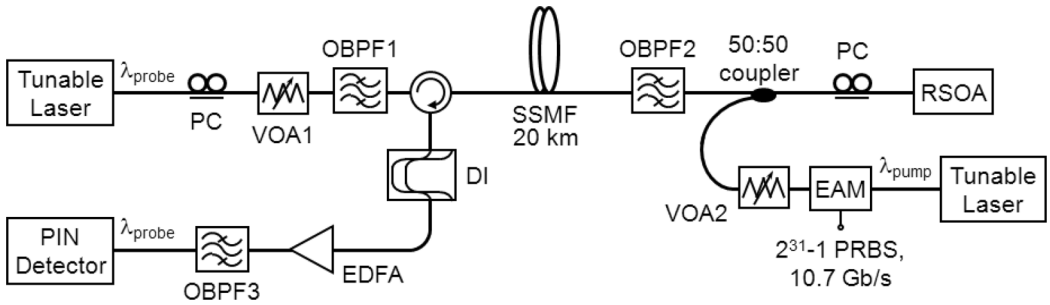

Fig. 2. Experimental setup. DI: delay interferometer, EAM: electroabsorption modulator, EDFA: Erbium-doped fiber amplifier, OBPF: optical band-pass filter, PC: polarization controller, PRBS: pseudo-random binary sequence, RSOA: reflective semiconductor optical amplifier, SSMF: standard single-mode fiber, and VOA: variable optical attenuator.

N-skip-M AWG, where N is the number of channels in each band and M is the number of lost channels between bands [22]. Alternatively, we can utilize the subcarrier multiplexing technique to separate the downstream data from the upstream data in the frequency domain. For example, the downstream data can be carried at a high subcarrier frequency of the probe light while the upstream data utilize the baseband modulation to avoid the spectral overlap [3].

It is worth noting that there is a potential in the future that the proposed transmitter, which is composed of an EML, a coupler, and an RSOA, could be integrated into a single monolithic chip to take advantage of semiconductor manufacturing technologies [23]. This will help to substantially lower the implementation cost of the proposed transmitters.

III. Experimental Demonstration and Discussion

A. Experimental Setup

We demonstrate the proposed colorless optical transmitter for WDM PON upstream transmission using the experimental setup depicted in Fig. 2. A tunable laser source provides a CW probe signal at $\lambda_{\mathrm{probe}} = 1560$ nm. We use a variable optical attenuator (VOA), VOA1, to adjust the power level of the probe signal. The CW probe signal is fed to an optical bandpass filter (OBPF), OBPF1, and then launched into SSMF before being sent to OBPF2. OBPF1 and OBPF2, which emulate the AWGs at the CO and the remote node, respectively, have a 3-dB bandwidth of 0.6 nm.

At the ONU side, we have a tunable laser followed by an EAM to simulate an EML. This is to allow tuning the wavelength of the pump signal and thus to study the conditions for colorless operation in the proposed scheme. Upstream NRZ data running at 10.7 Gb/s with a pseudo-random binary sequence (PRBS) length of $2^{31} - 1$ are fed to the EAM for intensity modulation. Here, we assume Reed-Solomon (255, 239) forward-error correction (FEC)-coded data with a 7% overhead. The extinction ratio (ER) of the pump signal is $\sim$10 dB. The power level of the pump signal is adjusted at the EAM output using VOA2. The pump and probe signals are then combined by a 50:50 optical coupler and launched into an RSOA for wavelength conversion. The RSOA used in the experiment is an uncooled device housed in a transistor outline package. It is DC-biased at 50 mA and no high-speed signal is applied. Under this bias condition, the 3-dB spectral width of the RSOA output is measured to be 33 nm, ranging from 1529 to 1562 nm. Unless stated otherwise, the optical powers of the pump and probe signals injected into the RSOA are set to be -10 and -16 dBm, respectively. The input saturation power of the RSOA, defined as the input optical power at which the signal gain is compressed by 3 dB from its small signal gain, is measured to be -22 dBm. Thus, the RSOA operates in the saturation region. Polarization controllers (PCs) are inserted at the inputs of VOA1 and the polarization-sensitive RSOA to maximize the seeding and conversion efficiencies. The RSOA used in the demonstration has a polarization-dependent gain of $\sim$20 dB. Although the pump signal can give rise to a nonlinear polarization rotation, a change in the polarization state of the probe signal in the presence of the pump signal [24], polarization-insensitive RSOAs can be used for real systems to eliminate the need for PCs. The output power of the wavelength-converted signal at 1560 nm is 2.5 dBm when the optical power of the injected pump signal at 1550 nm is -10 dBm.

The converted upstream signal at λ_{probe} is sent back to the CO over the same feeder fiber. The signal is then fed to a DI with an FSR of 16.1 GHz. We use an optically pre-amplified receiver comprising an Erbium-doped fiber amplifier (EDFA), OBPF3 ($\mathrm{bandwidth} = 0.6$ nm), and a PIN detector. The two optical filters on the upstream link, OBPF2 and OBPF3, suppress the pump signal by >50 dB when $|\lambda_{\mathrm{pump}} - \lambda_{\mathrm{probe}}| > 2$ nm.

B. Experimental Results

We first measure the optical spectra of the upstream signal before and after the DI, as shown in Fig. 3. Also shown in the figure is the transmittance curve of the DI. The peak wavelength of the DI transmittance is located 0.036 nm shorter than the upstream signal, which is fixed throughout the experiment. Thus, the DI serves to filter out the red-shifted chirp, which is induced by the refractive index modulation of the RSOA during the wavelength conversion [25]. This chirp tailoring created by the off-center filtering [16], [26] greatly improves the receiver sensitivity as well as the dispersion tolerance of the upstream signal, which will be shown later in this section.

Fig. 4 shows the measured bit-error ratio (BER) curves of the upstream signal. The pump and probe wavelengths are set to be 1550 and 1560 nm, respectively. The back-to-back receiver sensitivity (at a BER of 1.8×10^{-4}) is measured to be -32.4 dBm. In back-to-back operation, the 20-km fiber is replaced with an

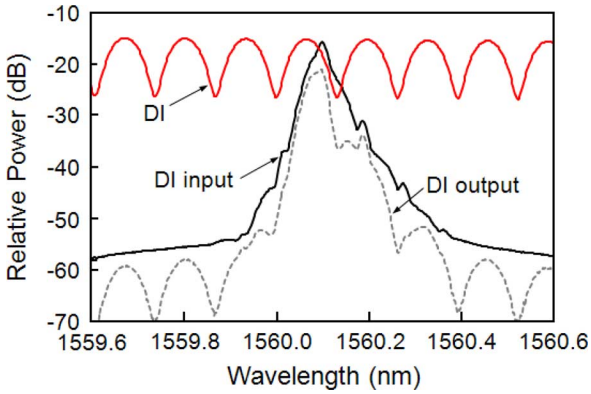

Fig. 3. Measured optical spectra at the DI input (solid black) and at the DI output (dashed grey). The transmittance curve of the DI is plotted in red.

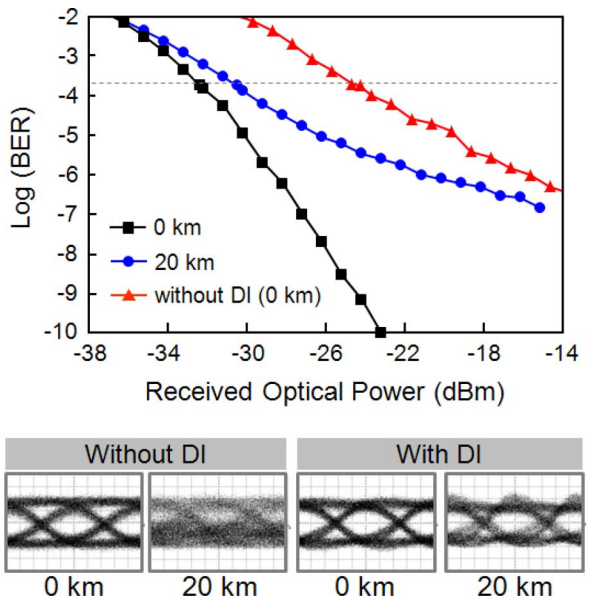

Fig. 4. Measured BER performance of the 10.7-Gb/s upstream signals when $\lambda_{\mathrm{pump}} = 1550$ nm and $\lambda_{\mathrm{probe}} = 1560$ nm. The insets show the received eye diagrams at the back-to-back and after 20-km transmission. The grey dotted line indicates the FEC threshold at a BER of 1.8×10^{-4}.

optical attenuator with the same loss. After 20-km transmission in the loop-back configuration, we observe an error floor at around 10^{-7} and the receiver sensitivity is degraded by 1.7 dB. This should be attributed to Rayleigh backscattering-induced crosstalk. We next remove the DI from the setup to investigate its effects on the BER performance. In back-to-back operation, the receiver sensitivity is measured to be -24.3 dBm, which is 8.1 dB worse than that with the DI. It is worth noting that we are not able to achieve the pattern synchronization for the BER measurement after 20-km transmission without the use of the DI. It is also evident from the eye diagrams in the insets of Fig. 4 that the DI significantly improves the eye opening. In the absence of the DI, the eye opening is completely closed after 20-km transmission.

To measure the gain recovery time of the RSOA, we setup an apparatus as shown in Fig. 5(a) [27]. A 60-ps pulsed pump signal at 1550 nm, as shown in Fig. 5(b), is first combined

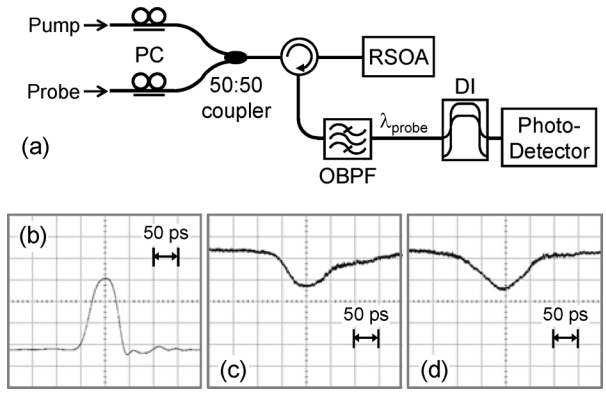

Fig. 5. (a) Experimental setup to measure the gain recovery time of the RSOA. (b) Waveform of the 60-ps pump signal. (c) Waveform of the probe signal before the DI. (d) Waveform of the probe signal after the DI.

with a CW probe signal at 1560 nm and then launched into the RSOA through an optical circulator. After the wavelength conversion, we filter out the pump signal using an OBPF having a 3-dB bandwidth of 0.6 nm. The DI is used at the output of the OBPF. The signal is detected with a high-speed detector. Fig. 5(c) shows the gain recovery of the RSOA in the absence of the DI. It shows the typical SOA gain recovery. The leading edge (i.e., falling edge) is determined by the pump pulse duration. The trailing edge (i.e., rising edge) is known to be governed by three different timescales [27]. Fast gain recovery on subpicosecond and a few picoseconds timescales driven by carrier-carrier scattering and carrier-phonon interactions, respectively [28] and slow gain recovery driven by electron-hole interactions on a nanosecond timescale. Due to the large pulse duration of the pump signal, the fast gain recovery on a picosecond timescale is not observed in Fig. 5(c), but the slow gain recovery is clearly observed. Fig. 5(d) shows the waveform of the probe signal in the presence of the DI. The DI suppresses the slow gain recovery components of the RSOA output signal, and thus the wavelength-converted signal recovers much faster than the gain recovery of the RSOA itself [27]. The improved bandwidth performance by use of the DI is also manifested through a modulated data pattern.

Fig. 6 shows the captured waveforms of the upstream signal before and after the DI at the back-to-back operation in Fig. 2. The bit pattern applied to the pump signal is '10011 01011'. The figure shows that due to the XGM-induced wavelength conversion we have an inverted bit pattern at the receiver. It also shows that the presence of the DI does not alter the bit pattern and we do not need a precoder in the proposed scheme. It is clear from Figs. 4 and 6 that the DI improves the eye opening, especially for the bit patterns which contain high-frequency components such as '101' and '010'. The thickness of both '1' and '0' rails is also reduced by the use of the DI. These are because of improved bandwidth of the wavelength conversion by the DI. In our experiment performed at 10.7 Gb/s, the rising/falling time of the converted signal is limited by the pulse width of the pump signal. Ultimately the bandwidth of the wavelength conversion would be limited by fast carrier dynamics of the RSOA such as carrier-carrier scattering and carrier-phonon interactions [27],

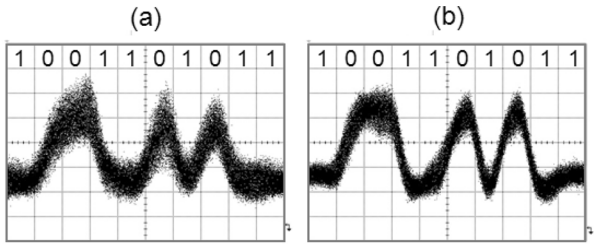

Fig. 6. Captured waveforms of the upstream signal in back-to-back operation (a) before the DI and (b) after the DI. The bit pattern applied is '10011 01011'.

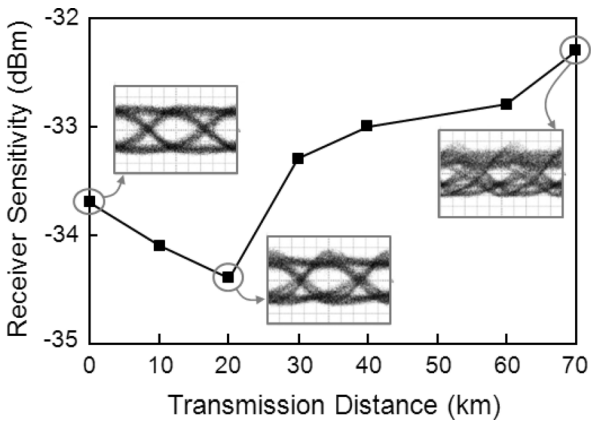

Fig. 7. Dispersion tolerance of the 10.7-Gb/s signal generated by the proposed transmitter. The insets are the eye diagrams measured at selected distances. In this measurement, the transmission fiber is moved between the circulator and the DI to exclude the Rayleigh backscattering-induced crosstalk.

[28]. Thus, it is expected that the proposed scheme could be potentially used for 20 Gb/s and beyond.

Fig. 7 shows the dispersion tolerance of the 10.7-Gb/s signal generated by the proposed transmitter. In this measurement, the transmission fiber is moved between the circulator and the DI in Fig. 2 to exclude the Rayleigh backscattering-induced crosstalk. This modified setup also allows us to keep the injection power of the CW probe signal unchanged over transmission distance. In back-to-back operation, the receiver sensitivity is measured to be -33.7 dBm. After transmission over 20-km SSMF, it is improved by 0.7 dB. In the proposed scheme, some amount of chromatic dispersion acts favorably on the system performance. This confirms that the 1.7-dB transmission penalty in Fig. 4 is caused by Rayleigh backscattering. The receiver sensitivity degrades after 20 km but we have only 1.4-dB dispersion penalty after transmission over 70-km SSMF. The high dispersion tolerance comes from the chirp tailoring of the DI.

To guarantee the colorless operation of the proposed scheme, the pump wavelength should be any arbitrary wavelength within the pump band. Thus, we measure the receiver sensitivity of the upstream signal while tuning the wavelength of the pump wavelength. Fig. 8 shows the receiver sensitivity as a function of the pump wavelength when the probe wavelength is set to 1560 nm. The 20-km SSMF is placed back in the loop-back configuration as shown in Fig. 2. Depending upon whether the pump wavelength is shorter or longer than the probe wavelength, we have wavelength up- or down-conversion. Fig. 8 shows that we have receiver sensitivity better than -30 dBm when the pump wavelength ranges from 1544 to 1558 nm and from 1562 to 1580

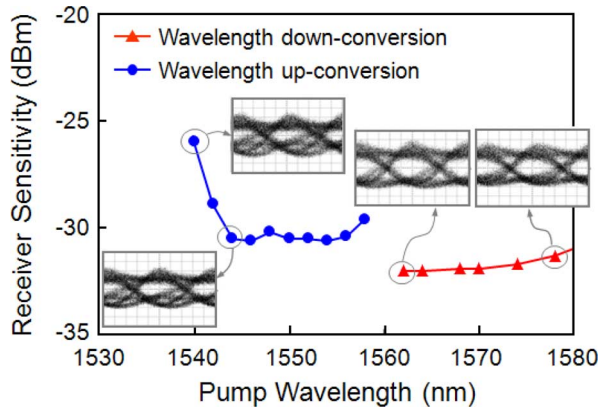

Fig. 8. Measured receiver sensitivity as a function of the pump wavelength when the probe wavelength is 1560 nm. The transmission distance is 20 km. The eye diagrams at selected pump wavelengths are shown in the insets.

nm. The minimum wavelength separation between the pump and probe signal is 2 nm to suppress the pump signal using the OBPFs on the link. One interesting observation in Fig. 8 is that the wavelength up-conversion underperforms the wavelength down-conversion by ~ 1.4 dB. This is due to the ER degradation in the case of wavelength up-conversion which is measured to be ~ 0.5 dB. This degradation is a result of the asymmetric gain compression due to the band-filling effects, which makes the ER always better for wavelength down-conversion [29]–[31]. It is found in Fig. 8 that as the pump wavelength increases, the receiver sensitivity for the wavelength down-conversion gradually degrades. This is because of the reduced gain of the RSOA beyond 1565 nm. Fig. 8 also shows that the receiver sensitivity degrades rapidly when the pump wavelength is below 1544 nm. This penalty is in part attributed to the bandwidth limitation of the EAM used in our experiment. The ER of the pump signal at the EAM output degrades by ~ 0.5 dB as the pump wavelength is tuned from 1544 to 1540 nm. The RSOA gain which is reduced by ~ 0.4 dB when the wavelength changes from 1544 to 1540 nm also contributes partly to this penalty.

Next, we fix the wavelength of the pump signal to 1550 nm and tune the wavelength of the probe signal. Fig. 9 shows the measured receiver sensitivity as a function of the probe wavelength. This is to investigate the bandwidth of the wavelength conversion when the pump wavelength is fixed, for example, at 1550 nm. In this measurement, as we tune the wavelength of the CW probe signal, the center wavelengths of OBPF1, OBPF2, and OBPF3 are tuned accordingly. The phase delay of the DI is also adjusted to minimize the BER. Similar to Fig. 8, the wavelength down-conversion outperforms the wavelength up-conversion. However, the performance of the wavelength up-conversion deteriorates further when the probe wavelength is longer than 1560 nm. This is due to the reduction in the gain of the EDFA utilized at the receiver. The limited tunability of the OBPFs used in our experiment does not allow us to measure the performance below 1532 nm.

The wavelength conversion efficiency is in general affected by the energy of the input signals. Fig. 10 shows the measured receiver sensitivity as we change the power of either the pump or the probe signal. The pump and probe wavelengths are set to be

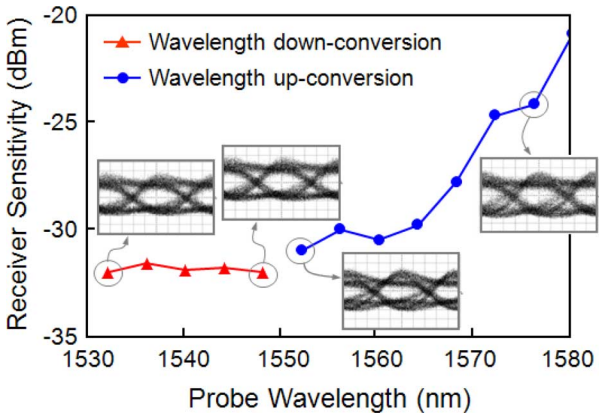

Fig. 9. Measured receiver sensitivity as a function of the probe wavelength when the pump wavelength is 1550 nm. The transmission distance is 20 km. The eye diagrams at selected probe wavelengths are shown in the insets.

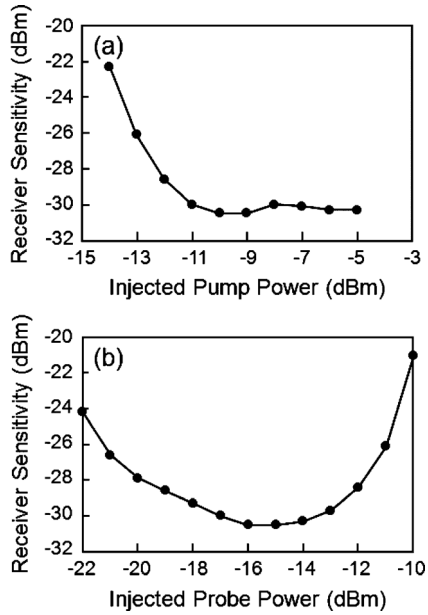

Fig. 10. (a) Measured receiver sensitivity as a function of the injected pump power into the RSOA when the probe power is -16 dBm. (b) Measured receiver sensitivity as a function of the injected probe power into the RSOA when the pump power is -10 dBm. The transmission distance is 20 km. λ_{pump} and λ_{probe} are 1550 and 1560 nm, respectively.

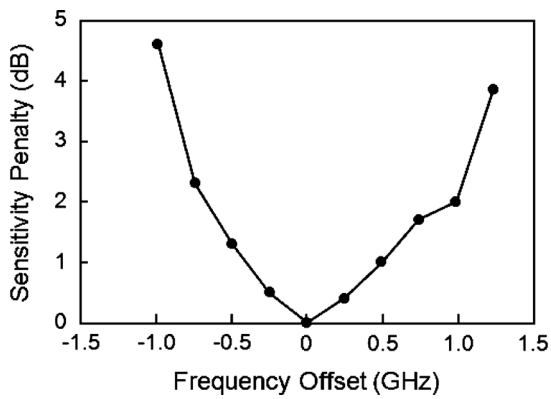

Fig. 11. Measured sensitivity penalty as a function of the frequency offset between the DI and the probe signal. The transmission distance is 20 km.

1550 and 1560 nm, respectively. The transmission distance is 20 km. Fig. 10(a) shows the receiver sensitivity versus the injected pump power into the RSOA when the probe power is -16 dBm. When the pump power is lower than -11 dBm, the pump power is not sufficient enough to operate the RSOA in a deep saturation region, inducing some sensitivity penalties. On the other hand, strong pump power improves the receiver sensitivity, leveling it off at around -30 dBm. The effect of the probe power on the system performance is plotted in Fig. 10(b). The pump power is fixed to -10 dBm in this figure. The result shows that we have an optimum range of injected probe power, which ranges from -19 to -12 dBm for 2-dB penalty window. When the injected probe power is lower than this range, the upstream signal suffers from low conversion efficiency and thus signal-to-noise degradation. On the other hand, strong probe power deteriorates the extinction ratio of the converted signal since the CW probe signal still saturates the RSOA when the pump signal is off (i.e., '0' bits) [32].

In a WDM-PON system using the proposed scheme, the injected pump power can be readily adjusted since both the EML and RSOA are located at the same place. Besides, as shown in Fig. 10(a), the required pump power for injection is > -11 dBm, which is translated into > -8 dBm at the output of the EML. This can be easily satisfied by using commercially available EMLs.

The power budget of a loop-back configured network can be limited either by the injection power requirements or the power difference between the available transmitter power and the receiver sensitivity. In our demonstration, we have a power difference of 33 dB [$= 2.5$ dBm (RSOA output power) $+30.5$ dBm (receiver sensitivity)]. On the other hand, the required optical power of the CW probe signal is -19 dBm. Therefore, the power budget of the WDM-PON system utilizing the proposed transmitter would be limited by the injection power requirement of the CW probe signal. With the fiber launch power of 6 dBm, the system can accommodate a total link loss of 25 dB $(= 6 + 19)$. Taking into account the loss of 20-km fiber (6 dB), an AWG (5 dB) at the remote node, and a 50:50 coupler (3 dB) at the ONU, we have a power margin of 11 dB.

Lastly, we measure the sensitivity penalties incurred by the frequency offset between the probe signal and DI. Fig. 11 shows the receiver sensitivity versus the frequency offset when the transmission distance is 20 km. Here, zero frequency offset refers to the case when the peak wavelength of the DI is located 0.036 nm shorter than the upstream signal, as shown in Fig. 3. It is found that the frequency offset should be kept within around ± 800 MHz to keep the penalty below 2 dB. In the proposed scheme, both the probe lasers and the DI are located at the CO. The frequency alignment can be readily achieved by frequency-locking the probe laser light to the DI, for example, using a servo loop [33].

IV. Conclusion

We have proposed and demonstrated a novel colorless optical transmitter based on all-optical wavelength conversion for upstream WDM-PON systems. The proposed optical transmitter at

the ONU side is composed of an electro-absorption modulated laser, an optical coupler, and a reflective semiconductor optical amplifier. Thus, it could be implemented potentially in a cost-effective manner through monolithic integration. A gain-saturated RSOA is used to imprint, through cross-gain modulation, the upstream data generated by the EML onto the continuous-wave seed light provided from the central office. An optical delay interferometer at the central office tailors the chirp of the converted upstream signal to improve the system bandwidth and the dispersion tolerance. Our experimental demonstration performed at 10.7 Gb/s shows that the proposed scheme works over 30 nm of either the pump (i.e., EML output) or probe (i.e., seed light) wavelength. Therefore, the proposed optical transmitter operates in a colorless manner since the EML wavelength can be chosen arbitrarily within this wavelength range.

Unlike other colorless optical transmitters based on directly modulated semiconductor opto-electronic devices, the modulation bandwidth of which is limited by the carrier life time in the active layer, the performance of the proposed transmitter is limited by fast carrier dynamics of the RSOA. Thus, we expect the proposed scheme could be used as an alternative solution to reflective electroabsorption modulator-SOA-based transmitter to implement high-capacity WDM PONs operating at 10 Gb/s/channel and beyond [34].

REFERENCES

[1] U. Hilbk, T. Hermes, J. Saniter, and F.-J. Westphal, "High capacity WDM overlay on a passive optical network," *Electron. Lett.*, vol. 32, no. 23, pp. 2162–2163, 1996.

[2] E. Wong, K. L. Lee, and T. B. Anderson, "Directly modulated self-seeding reflective semiconductor optical amplifiers as colorless transmitters in wavelength division multiplexed passive optical networks," *J. Lightw. Technol.*, vol. 25, no. 1, pp. 67–74, 2007.

[3] Z. Al-Qazwini and H. Kim, "Symmetric 10-Gb/s WDM-PON using directly modulated lasers for downlink and RSOAs for uplink," *J. Lightw. Technol.*, vol. 30, no. 12, pp. 1891–1899, June 2012.

[4] H. D. Kim, S.-G. Kang, and C.-H. Lee, "A low-cost WDM source with an ASE injected Fabry-Perot semiconductor laser," *IEEE Photon. Technol. Lett.*, vol. 12, no. 8, pp. 1067–1069, Aug. 2000.

[5] P. Healey, P. Townsend, C. Ford, L. Johnston, P. Townley, I. Lealman, L. Rivers, S. Perrin, and R. Moore, "Spectral slicing WDM-PON using wavelength-seeded reflective SOAs," *Electron. Lett.*, vol. 37, no. 19, pp. 1181–1182, Sept. 2001.

[6] Y. Takushima, K. Y. Cho, and Y. C. Chung, "Design issues in RSOA-based WDM PON," in *Proc. Photonics Global*, 2008, pp. C-34–C-37.

[7] G. Valicourt, D. Make, C. Fortin, A. Enard, F. V. Dijk, and R. Brenot, "10 Gbit/s modulation of reflective SOA without any electronic processing," in *Proc. OFC*, 2011, Paper OThT2.

[8] M. Omella, V. Polo, J. Lazaro, B. Schrenk, and J. Prat, "10 Gb/s RSOA transmission by direct duobinary modulation," in *Proc. ECOC*, 2008, Paper Tu.3.E.4.

[9] T. Duong, N. Genay, P. Chanclou, B. Charbonnier, A. Pizziant, and R. Brenot, "Experimental demonstration of 10 Gbit/s upstream transmission by remote modulation of 1 GHz RSOA using adaptively modulated optical OFDM for WDM-PON single fiber architecture," in *Proc. ECOC*, 2008, Paper Th.3.F.1.

[10] J. Wei, E. Hugues-Salas, R. Giddings, X. Jin, X. Zheng, S. Mansoor, and J. Tang, "Wavelength reused bidirectional transmission of adaptively modulated optical OFDM signals in WDM-PONs incorporating SOA and RSOA intensity modulators," *Opt. Exp.*, vol. 18, no. 10, pp. 9791–9808, May 2010.

[11] K. Y. Cho, Y. Takushima, and Y. C. Chung, "Enhanced chromatic dispersion tolerance of 11-Gb/s RSOA-based WDM PON using 4-ary PAM signal," *Electron. Lett.*, vol. 46, no. 22, pp. 1510–1512, Oct. 2010.

[12] K. Y. Cho, Y. Takushima, and Y. C. Chung, "10-Gb/s operation of RSOA for WDM PON," *IEEE Photon. Technol. Lett.*, vol. 20, no. 18, pp. 1533–1535, Sep. 2008.

[13] A. Agata and Y. Horiuchi, "RSOA-based 10 G WDM PON using FEC and MLSE equalizers," in *Proc. OFC*, 2010, paper OWG3.

[14] Q. Guo, A. V. Tran, and C.-J. Chae, "10-Gb/s WDM-PON based on low-bandwidth RSOA using partial response equalization," *IEEE Photon. Technol. Lett.*, vol. 23, no. 20, pp. 1442–1444, Oct. 2011.

[15] I. Papagiannakis, M. Omella, D. Klonidis, A. Birbas, J. Kikidis, I. Tomkos, and J. Prat, "Investigation of 10-Gb/s RSOA-based upstream transmission in WDM-PONs utilizing optical filtering and electronic equalization," *IEEE Photon. Technol. Lett.*, vol. 20, no. 24, pp. 2168–2170, Dec. 2008.

[16] H. Kim, "10-Gb/s operation of RSOA using a delay interferometer," *IEEE Photon. Technol. Lett*, vol. 22, no. 18, pp. 1379–1381, Sep. 2010.

[17] B. Glance, J. M. Wiesenfeld, U. Koren, A. H. Gnauck, H. M. Presby, and A. Jourdan, "High performance optical wavelength shifter," *Electron. Lett.*, vol. 28, no. 18, pp. 1714–1715, 1992.

[18] T. Durhuus, C. Joergensen, B. Mikkelsen, R. J. S. Pedersen, and K. E. Stubkjaer, "All optical wavelength conversion by SOA's in a Mach-Zehnder configuration," *IEEE Photon. Technol. Lett.*, vol. 6, no. 1, pp. 53–55, Jan. 1994.

[19] T. Durhuus, B. Mikkelsen, C. Joergensen, S. L. Danielsen, and K. E. Stubkjaer, "All-optical wavelength conversion by semiconductor optical amplifiers," *J. Lightw. Technol.*, vol. 14, no. 6, pp. 942–954, 1996.

[20] H. Kim, "Transmission of 10-Gb/s directly modulated RSOA signals in single-fiber loopback WDM PONs," *IEEE Photon. Technol. Lett.*, vol. 23, no. 14, pp. 965–967, 2011.

[21] [Online]. Available: http://www.gemfire.com/Main/Products/prod-pdfs.html

[22] S. Chandrasekhar, C. R. Doerr, and L. L. Buhl, "Flexible waveband optical networking without guard bands using novel 8-skip-0 banding filters," *IEEE Photon. Technol. Lett.*, vol. 17, no. 3, pp. 579–581, Mar. 2005.

[23] U. Koren, B. I. Miller, M. G. Young, M. Chien, G. Raybon, T. Brenner, R. Ben-Michael, K. Dreyer, and R. J. Capik, "A polarization insensitive optical amplifier with integrated electroabsorption modulators," *Electron. Lett.*, vol. 32, no. 1, pp. 111–113, Jan. 1996.

[24] H. Dorren, D. Lenstra, Y. Liu, M. Hill, and G.-D. Khoe, "Nonlinear polarization rotation in semiconductor optical amplifiers: Theory and application to all-optical flip-flop memories," *IEEE J. Quantum Electron*, vol. 39, no. 1, pp. 141–148, Jan. 2003.

[25] H. Kim, "A dual-detector optical receiver for WDM PON utilizing directly modulated RSOAs and delay interferometer," *IEEE Photon. Technol. Lett.*, vol. 23, no. 22, pp. 1733–1735, Nov. 2011.

[26] K. E. Zoiros, Z. V. Rizou, and M. J. Connelly, "On the compensation of chirp induced from semiconductor optical amplifier on RZ data using optical delay interferometer," *Opt. Comm.*, vol. 284, pp. 3539–3547, 2011.

[27] Y. Lin, E. Tangdiongga, Z. Li, S. Zhang, H. de Waardt, G. D. Khoe, and H. Dorren, "Error-free all-optical wavelength conversion at 160 Gb/s using a semiconductor optical amplifier and an optical bandpass filter," *J. Lightw. Technol.*, vol. 24, no. 1, pp. 230–236, Jan. 2006.

[28] J. Mark and J. Mork, "Subpicosecond gain dynamics in InGaAsP optical amplifiers: Experiment and theory," *Appl. Phy. Lett.*, vol. 61, no. 19, pp. 2281–2283, Nov. 1992.

[29] L.-Q. Guo and M. J. Connelly, "A novel approach to all-optical wavelength conversion by utilizing a reflective semiconductor optical amplifier in a co-propagation scheme," *Opt. Commun.*, vol. 281, no. 17, pp. 4470–4473, 2008.

[30] L.-Q. Guo and M. J. Connelly, "Signal-induced birefringence and dichroism in a tensile-strained bulk semiconductor optical amplifier and its application to wavelength conversion," *J. Lightw. Technol.*, vol. 23, no. 12, pp. 4037–4045, Dec. 2005.

[31] J. M. Wiesenfeld, "Gain dynamics and associated nonlinearities in semiconductor optical amplifiers," *Int. J. High Speed Electron.*, vol. 7, no. 1, pp. 179–222, 1996.

[32] K.-I. Chung, T.-Y. Kim, and S.-K. Han, "Analysis of all optical cascaded XGM wavelength converter using CW-holding beam," *Opt. Quantum Electron.*, vol. 34, no. 10, pp. 937–950, 2002.

[33] J. H. Jang, S. K. Shin, H. Kim, K. S. Lee, K. J. Park, and Y. C. Chung, "A cold-start WDM system using a synchronized etalon filter," *IEEE Photon. Technol. Lett.*, vol. 9, no. 3, pp. 383–385, Mar. 1997.

[34] G. Berrettini, G. Meloni, L. Giorgi, F. Ponzini, F. Cavaliere, P. Ghiggino, L. Poti, and A. Bogoni, "Colorless WDM-PON architecture for Rayleigh backscattering and path-loss degradation mitigation," *IEEE Photon. Technol. Lett.*, vol. 21, no. 7, pp. 453–455, Apr. 2009.

Author biographies not included by author request due to space constraints.